KSCE Journal of Civil Engineering (2013) 17(1):192-201
DOI 10.1007/s12205-013-1606-0

Structural Engineering
www.springer.com/12205

Nonlinear Winkler-based Beam Element with Improved Displacement Shape Functions

Suchart Limkatanyu*, Kittisak Kuntiyawichai, Enrico Spacone***, and Minho Kwon******

Received June 15, 2011/Accepted April 8, 2012

Abstract

This paper presents a Winkler-based beam element capable of representing the nonlinear interaction mechanics between the beam and the foundation. The element is derived based on a displacement-based formulation using improved displacement shape functions. The improved displacement shape functions are analytically derived based on the homogeneous solution to the governing differential equilibrium equation of the problem, thus enhancing the model accuracy. An iterative technique is used to determine the length-scale parameter needed in evaluating the displacement shape functions. Two numerical examples are used to verify the accuracy and the efficiency of the proposed Winkler-based beam model.

Keywords: *beam elements, Winkler foundation, finite element, stiffness-based formulation, virtual displacement principle, soil-structure interaction, nonlinear analysis*

1. Introduction

The problem of beams on flexible foundation is considered a classic example in which the interaction mechanics between the beams and the foundation plays an essential role in modeling the system. Several mathematical models with different degrees of complexity have been developed in literatures to represent the foundation flexibility. Generally, these mathematical models can be grouped broadly into two categories: continuum model and spring model (Selvadurai, 1979). In the continuum model, the foundation flexibility is taken into account by considering the foundation as a homogeneous semi-infinite elastic body (Mindlin, 1936; Reissner, 1967). Contrastingly, in the spring model, the foundation flexibility is accounted for by considering the foundation as a set of continuous springs (Winkler, 1867; Kerr, 1965; Valsov and Leontiev, 1966). Due to the complexity of solutions to boundary value problems using the continuum model, the continuous-spring model has been used extensively by geotechnical researchers and engineers to represent the soil-structure interaction mechanics (e.g., Eisenberger and Yankelevsky, 1985; Gendy and Saleeb, 1999; Lee *et al*., 2003; Taciroglu *et al*., 2006; Celep and Demir, 2007; Zhang *et al*., 2009; Kim and Chung, 2009; Kim and Yang, 2010; Chore *et al*., 2010; Sapountzakis and Kampitsis, 2010; Raychowdhury, 2011; Limkatanyu *et al.*, 2012). The Winkler foundation model (Winkler, 1867) has been the simplest and most widely used spring model and is often referred to as the "*one-parameter*" foundation model. In the Winkler foundation model, reactive forces of the foundation are assumed to be proportional at every point to the deflection of the beam at that point. Besides the soil-structure interaction problems, the beam-Winkler foundation model can be used to simulate behaviors of several engineering problems, for example, the dowel action for shear transfer in cracked concrete (He and Kwan, 2001), torsion of stiffened open thin-walled steel sections (Gosowski, 2007), vibration of carbon nanotubes (Wang and Chen, 2010), mode-I delamination in multi-directional laminated composites (Shokrieh and Heidari-Rarani, 2011), etc. It is worthwhile to mention that several researchers have recently used more refined foundation spring models to represent the soil-structure interaction mechanics. For examples, Ma *et al.* (2009) and Mullapudi and Ayoub (2010) used the two-parameter foundation model to account for the soil continuity while Avramidis and Morfidis (2006), Zhang (2009), and Sapountzakis and Kampitsis (2011a, 2011b) employed the three-parameter foundation model to account for the soil continuity as well as to determine the level of the vertical-displacement continuity at the boundaries between the loaded and unloaded soil surfaces. Apart from the monograph on the closed-form solutions to the problems

*Associate Professor, Dept. of Civil Engineering, Faculty of Engineering, Prince of Songkla University, Songkhla 90112, Thailand (Corresponding Author, E-mail: suchart.l@psu.ac.th)
**Associate Professor, Dept. of Civil Engineering, Faculty of Engineering, Ubonratchathani University, Ubonratchathani 34190, Thailand (E-mail: kittisak.ubu@gmail.com)
***Professor, Dept. PRICOS, Faculty of Architecture, University "G. D'Annunzio", Pescara 65129, Italy (E-mail: e.spacone@unich.it)
****Associate Professor, Dept. of Civil Engineering, ERI, Gyeongsang National University, Jinju 660-701, Korea (E-mail: saburida@gmail.com)

by Hetenyi (1946), several numerical techniques have been used to solve the problems. The finite difference method was used by several researchers (e.g. Matlock and Reese, 1960) to solve for numerical solutions to the problems. However, this numerical technique had become obsolete some decades ago due to the emergence of its counterpart, the finite element method.

The displacement-based finite element method has been widely used as a numerical tool to solve the problems of beams on Winkler foundation. The simplest way to account for the foundation contribution is to attach discrete foundation springs at the nodes of the conventional beam element (e.g. Bowles, 1974; Harden and Hutchinson, 2009, etc.). However, the model accuracy is hampered by the replacement of continuous foundation springs with discrete ones. A more elegant way to include the foundation effects is to smear the foundation all over the element length. Several researchers have followed this approach to account for the foundation effects. Tong and Rossettos (1977) formulated the beam-foundation element using Hermite displacement interpolation functions. Limkatanyu and Spacone (2006) used the same approach to develop the nonlinear Winkler-based beam element. Due to the assumed nature of displacement shape functions, the model accuracy was still limited. To eliminate the approximate nature inherent in Hermite displacement shape functions, several researchers (Miranda and Nair, 1966; Ting and Mockry, 1984; Eisenberger and Yankelevsky, 1985) have derived the "exact" element stiffness matrix using the method of initial parameters to express the solution of the fourth-order differential equation in terms of four response quantities; i.e. deflection, rotation, shear, and moment. However, these beam-foundation models can be applied only to a linear elastic beam-foundation system. In recent years, the Performance-Based Seismic Design Methodology (SEAOC. Vision 2000, 1995) has been adopted. In this design methodology, it urges structural engineers to utilize the beneficial effects from the nonlinear soil-structure interaction to reduce the structural force and ductility demands. These beneficial effects are resulted from mobilization of the foundation ultimate capacity and its mechanism for dissipating seismic energy (e.g., shallow foundation rocking). Consequently, development of the nonlinear Winkler-based beam model is an important step toward implementation of the newly proposed Performance-Based Seismic Design Methodology.

The main objective of this paper is to propose a more accurate nonlinear Winkler-based beam model. This beam model stems from the displacement-based model developed by Limkatanyu and Spacone (2006). The Winkler-based beam model presented in the present study differs from that presented in Limkatanyu and Spacone (2006) in that the displacement shape functions are analytically derived based on the homogeneous solution to the governing differential equilibrium equation, thus resulting in a more accurate Winkler-based beam model. The formulation of the Winkler-based beam element is based on the virtual displacement principle. Two numerical examples are used to verify the accuracy and the efficiency of the proposed beam model. The first example is used to perform the convergence studies of the proposed model and to show its accuracy in representing both global and local responses. The second example is used to demonstrate the capability of the proposed beam element to trace the softening response and to study the internal-force redistribution nature inherent to the beam-foundation system. All symbolic calculations throughout this paper are performed using the computer software Mathematica (Wolfram, 1992) and the resulting beam-foundation model is implemented in the general-purpose finite element platform FEAP (Taylor, 2000).

2. Definitions

In the present study, the proposed Winkler-based beam element shown in Fig. 1 comprises of the following sub-components: a 2-node beam, plus smeared foundation springs representing the supporting deformable medium (e.g., soil).

Following the notation of Fig. 1, the element nodal displacements are:

$$\mathbf{U} = \{\mathbf{U}^1 | \mathbf{U}^2\}^T \tag{1}$$

where $\mathbf{U}^1 = \{U_1^1\ U_2^1\}^T$ and $\mathbf{U}^2 = \{U_1^2\ U_2^2\}^T$ are arrays containing the displacements at node 1 and 2, respectively. Their work-conjugate nodal forces are grouped in the element force vector $\mathbf{P} = \{\mathbf{P}^1 | \mathbf{P}^2\}^T$.

The transverse displacement $v_B(x)$ of the beam section is grouped in the following array:

$$\mathbf{u}(x) = \{v_B(x)\} \tag{2}$$

The sectional curvature $\kappa_B(x)$ is grouped in the following array:

$$d_B(x) = \{\kappa_B(x)\} \tag{3}$$

Since the kinematics of the beam section is described based on the Euler-Bernoulli beam theory, sectional shear deformation vanishes in this beam theory. However, the sectional shear force can be determined using equilibrium conditions and makes no contribution to the model formulation. Following the infinitesimal deformation assumption, the sectional curvature is related to the transverse displacement through the compatibility relation $\kappa_B(x) = d^2 v_B / dx^2$. For the ease of model implementation, the following matrix notion is used:

$$\mathrm{d}_B(x) = \partial_B \mathbf{u}(x) \tag{4}$$

where ∂_B is a linear differential operator defined as:

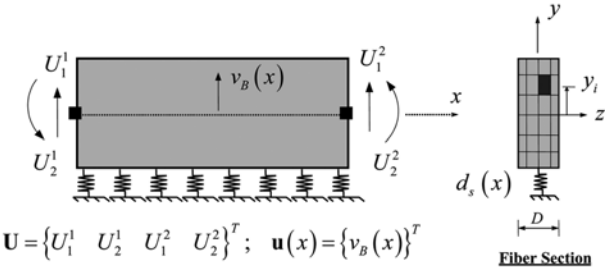

Fig. 1. A 2-Node Winkler-Based Beam Element

$$\partial_B = \left[\frac{d^2}{dx^2}\right] \tag{5}$$

The sectional moment $M_B(x)$ work-conjugate pair of $\kappa_B(x)$ is grouped in the array $\mathbf{D}_B(x)$ defined as:

$$\mathbf{D}_B(x) = \{M_B(x)\} \tag{6}$$

The foundation deformation $d_s(x)$ is of interest in the formulation and is grouped in the following array:

$$\mathbf{d}_s(x) = \{d_s(x)\} \tag{7}$$

Following the Winkler foundation theory, which assumes perfect compatibility between beam and foundation displacements, the foundation deformation is determined through the following compatibility relation:

$$d_s(x) = v_B(x) \tag{8}$$

In matrix notation, the foundation compatibility relation of Eq. (8) is written as:

$$\mathbf{d}_s(x) = \partial_s \mathbf{u}(x) \tag{9}$$

where ∂_s is a transformation matrix defined as:

$$\partial_s = [1] \tag{10}$$

Finally, the foundation force $D_s(x)$, conjugate work pair of $d_s(x)$, is grouped in the array $\mathbf{D}_s(x)$:

$$\mathbf{D}_s(x) = \{D_s(x)\} \tag{11}$$

3. Displacement Formulation of Winkler-Based Beam Element

In the displacement-based model, the virtual displacement principle forms the core of the formulation and the element displacement $\mathbf{u}(x)$ is expressed as functions of the element nodal displacements $\mathbf{U}$ through the displacement shape function matrix $\mathbf{N}_B(x)$:

$$\mathbf{u}(x) = \mathbf{N}_B(x)\mathbf{U} \tag{12}$$

The displacement shape functions in $\mathbf{N}_B(x)$ are obtained by solving analytically the governing differential equilibrium equation as shall be discussed later.

3.1 Compatibility

In the displacement-based formulation, the beam and foundation compatibility conditions are both enforced in the strong sense. Thus, the beam-section and foundation deformations are directly related to the element nodal displacements $\mathbf{U}$ through the following equations:

$$\mathbf{d}_B(x) = \mathbf{B}_B(x)\mathbf{U}$$
$$\mathbf{d}_s(x) = \mathbf{B}_s(x)\mathbf{U} \tag{13}$$

where the beam $\mathbf{B}_B(x)$ and the foundation $\mathbf{B}_s(x)$ deformation-displacement matrices are defined as:

$$\mathbf{B}_B(x) = \partial_B \mathbf{N}_B(x) \text{ and } \mathbf{B}_s(x) = \partial_s \mathbf{N}_B(x) \tag{14}$$

3.2 Material Constitutive Laws: Beam Section and Foundation

The sectional moment $M(x)$ and curvature $\kappa(x)$ are related by a nonlinear deformation-based constitutive model:

$$M(x) = \Psi[\kappa(x)] \text{ or } \mathbf{D}_B(x) = \Psi[d_B(x)] \tag{15}$$

In the present work, the fiber section model with nonlinear uniaxial stress-strain laws for the constituent materials is used to derive the nonlinear function in Eq. (15). The foundation force $D_s(x)$ and deformation $d_s(x)$ are related by a nonlinear deformation-based constitutive model:

$$D_s(x) = \Xi[d_s(x)] \text{ or } D_s(x) = \Xi[\mathbf{d}_s(x)] \tag{16}$$

The nonlinear force-deformation relations for the beam section and foundation can be written in consistent linearized matrix forms as:

$$\mathbf{D}_B(x) = \mathbf{D}_B^0(x) + \mathbf{k}_B \Delta\mathbf{d}_B(x)$$
$$\mathbf{D}_s(x) = \mathbf{D}_s^0(x) + \mathbf{k}_s \Delta\mathbf{d}_s(x) \tag{17}$$

where $\mathbf{D}_B^0(x)$ and $\mathbf{D}_s^0(x)$ are the initial beam-section and foundation forces, respectively; $\mathbf{k}_B(x)$ is the beam-section tangent stiffness matrix; and $\mathbf{k}_s(x)$ is the matrix containing the foundation tangent stiffness.

3.3 Equilibrium: The Virtual Displacement Principle

In the displacement-based formulation, the element equilibrium is imposed in a weak sense. Applying the virtual displacement principle, substituting Eq. (13), and subsequently imposing the arbitrariness of the virtual nodal displacements $\delta\mathbf{U}$ result in the following weak equilibrium statement:

$$\int_L \mathbf{B}_B^T(x)\mathbf{D}_B(x)dx + \int_L \mathbf{B}_s^T(x)\mathbf{D}_s(x)dx = \mathbf{P} \tag{18}$$

Substitution of Eqs. (17) into (18) yields the incremental form of equilibrium as:

$$(\mathbf{K}_B + \mathbf{K}_s)\Delta\mathbf{U} = \mathbf{P} - (\mathbf{P}_B^0 + \mathbf{P}_s^0) \tag{19}$$

where,

$\mathbf{K}_B = \int_L \mathbf{B}_B^T(x)\mathbf{k}_B(x)\mathbf{B}_B(x)dx$: The beam element stiffness matrix

$\mathbf{K}_s = \int_L \mathbf{B}_s^T(x)\mathbf{k}_s(x)\mathbf{B}_s(x)dx$: The Winkler foundation element stiffness matrix

$\mathbf{P}_B^0 = \int_L \mathbf{B}_B^T(x)\mathbf{D}_B^0(x)dx$: The beam element resistant force vector

$\mathbf{P}_s^0 = \int_L \mathbf{B}_s^T(x)\mathbf{D}_s^0(x)dx$: The Winkler foundation element resistant force vector.

4. Improved Displacement Shape Functions

The differential equation for the transverse displacement of a beam-Winkler foundation system shown in Fig. 2 (Pilkey, 2007) is:

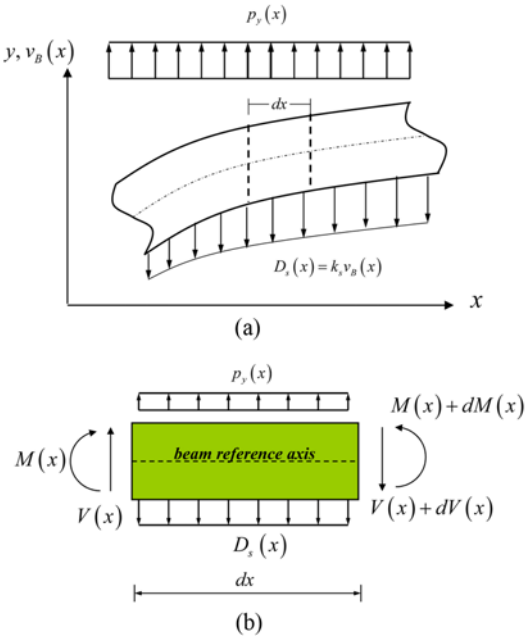

Fig. 2. (a) A Beam on Winkler Foundation, (b) A Differential Segment Cut from the Beam

$$k_B \frac{d^4 v_B(x)}{dx^4} + k_s v_B(x) + p_y(x) = 0 \tag{20}$$

where k_B is the flexural rigidity of the beam section; k_s is the foundation stiffness; and $p_y(x)$ is the applied distributed load.

The improved displacement shape functions are obtained by solving the governing differential equilibrium equation of Eq. (20). The homogeneous solution of Eq. (20) for $p_y(x)$=0 is:

$$v_B(x) = \gamma_1 c_1 + \gamma_2 c_2 + \gamma_3 c_3 + \gamma_4 c_4 \tag{21}$$

where the length-scale parameter $\lambda = \sqrt[4]{k_s / 4k_B}$ represents the inverse of a characteristic length; c_1 to c_4 are generalized coordinates to be determined from geometric boundary conditions; and γ_1 to γ_4 are hyperbolic-trigonometric base functions listed below:

$$\gamma_1 = e^{-\lambda x}\cos\lambda x;\ \ \gamma_2 = e^{-\lambda x}\sin\lambda x;\ \ \gamma_3 = e^{\lambda x}\cos\lambda x;\ \text{and}$$
$$\gamma_4 = e^{\lambda x}\sin\lambda x \tag{22}$$

In matrix form, Eq. (21) can be written as:

$$v_B(x) = \Gamma^T \mathbf{C} \tag{23}$$

where $\mathbf{\Gamma}$ and $\mathbf{C}$ are column vectors containing γ_1 to γ_4 and c_1 to c_4, respectively. The four geometric boundary conditions are related to element nodal displacements as:

$$v_B\big|_{x=0} = U_1^1 ;\ \left.\frac{dv_B}{dx}\right|_{x=0} = U_2^1 ;\ v_B\big|_{x=L} = U_1^2 ;\ \text{and}$$
$$\left.\frac{dv_B}{dx}\right|_{x=L} = U_2^2 \tag{24}$$

Substituting for $v_B(x)$ and its derivatives from Eqs. (23) into (24) yields the following algebraic relation:

$$\mathbf{U} = \mathbf{T}\mathbf{C} \tag{25}$$

where $\mathbf{T}$ is the mapping matrix between the generalized coordinates and the element nodal displacements. Symbolically solving Eq. (25) and subsequently substituting into Eq. (23), we have:

$$v_B(x) = \Gamma^T \mathbf{T}^{-1} \mathbf{U} = \mathbf{N}_B(x)\mathbf{U} \tag{26}$$

where $\mathbf{N}_B(x) = \lfloor N_{B1}(x)\ N_{B2}(x)\ N_{B3}(x)\ N_{B4}(x) \rfloor$ is an array containing the improved displacement shape functions. The expression of each displacement shape function is given in Appendix A. It is noted that $\mathbf{N}_B(x)$ becomes the cubic polynomial shape functions for beams without supporting foundation when the length-scale parameter λ approaches zero and are "*exact*" displacement shape functions for a linear beam-foundation system.

Following the nonlinear nature of beam-section and foundation constitutive laws, the beam-section flexural rigidity k_B and foundation stiffness k_s may not be constant. Therefore, the length-scale parameter λ can be varied with the loading magnitudes. An iterative technique is used to determine the length-scale parameter needed in evaluating the displacement shape functions. In the present work, two following schemes are proposed to determine the average value of λ used in evaluating $\mathbf{N}_B(x)$ at each loading step of the nonlinear solution algorithm. In the first scheme, the average length-scale parameter λ^{ave} is computed as follows:

$$\lambda^{ave} = \sum_{i=1}^{NIP} \frac{\lambda_i w_i}{L} \tag{27}$$

where w_i is the weight of integration-point i and NIP is the number of integration points. In the second scheme, the average values of k_B and k_s are first computed and then λ^{ave} is computed as:

$$\lambda^{ave} = \sqrt[4]{\frac{k_s^{ave}}{4k_B^{ave}}} \tag{28}$$

where $k_B^{ave} = \sum_{i=1}^{NIP} \frac{k_{Bi} w_i}{L}$ and $k_s^{ave} = \sum_{i=1}^{NIP} \frac{k_{si} w_i}{L}$.

5. Model Evaluation by Numerical Examples

Two numerical examples are exemplified to verify the accuracy and to demonstrate the capabilities of the proposed nonlinear Winkler-based beam element. The first numerical example is a simply supported beam on hardening foundation. The second numerical example is a free-free beam on softening foundation subjected to an imposed displacement at its midspan.

5.1 Example I: Global and Local Convergence Studies

The simply supported beam on hardening foundation shown in Fig. 3 was used by Limkatanyu and Spacone (2006) to compare the convergence, accuracy, and characteristics of three finite element formulations: displacement-based, mixed, and force-hybrid models. To ease the convergence studies in the present work, this numerical example is also employed to evaluate and

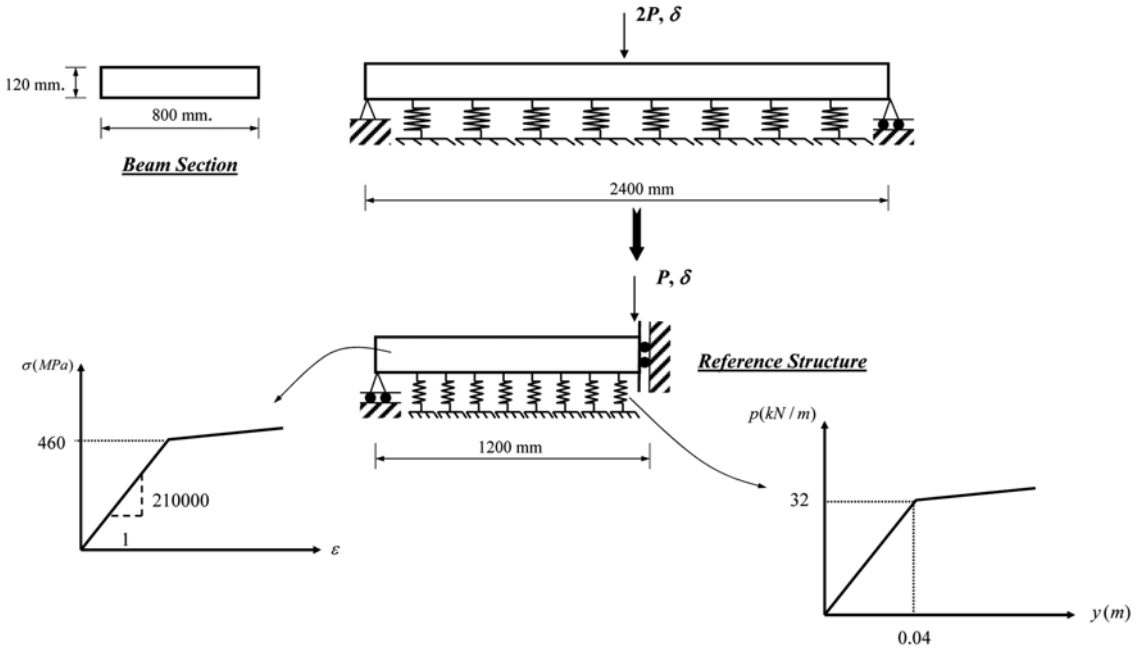

Fig. 3. Example I: Simply Supported Beam on Deformable Foundation

show the performance and efficiency of the proposed Winkler-based beam element. Only half of the beam is modeled due to symmetry. The characteristics of the beam and section geometry are shown in Fig. 3. The beam section is discretized into 20 fibers to represent the nonlinear sectional force-deformation response. Each fiber has a bilinear hardening constitutive relation with initial modulus of 210 GPa, yield strength of 460 MPa, and strain-hardening ratio of 0.01. The foundation force-deformation response is also assumed to be bilinear hardening with yield force of 32 kN/m, yield displacement of 0.04 m, and displacement-hardening ratio of 0.005.

Figure 4 compares the numbers of elements needed to obtain the converged global response for the two displacement-based elements proposed in the present work and in Limkatanyu and Spacone (2006). It is noted that the displacement-based model presented in the present work differs from that presented in Limkatanyu and Spacone (2006) in that the displacement shape functions used in the proposed model are analytically derived as discussed earlier while those used in Limkatanyu and Spacone (2006) are assumed to be cubic Hermitian polynomial, thus resulting in the approximate curvature interpolation functions. The two plots show the load-midspan displacement (P-δ) responses. A mesh consisting of 32 displacement-based elements with cubic Hermitian polynomials is used to obtain the so-called "*benchmark*" response. Five and seven Gauss-Lobatto integration points are assumed for each element of beam models presented in Limkatanyu and Spacone (2006) and in the present work, respectively. Larger numbers of integration points were used and did not change the responses. It is imperative to mention that the reason why the integration-point number required in the proposed model is more than that needed in the beam model of Limkatanyu and Spacone (2006) is due the more complex nature

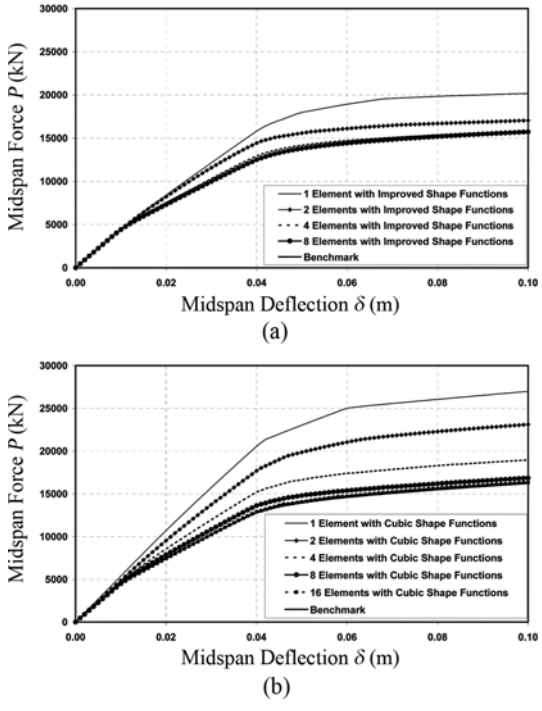

Fig. 4. Global Convergence Studies of the Two Winkler-Based Beam Models: (a) Model with Improved Displacement Shape Functions; (b) Model with Cubic Shape Functions

of hyperbolic-trigonometric displacement shape functions as compared to cubic polynomial shape functions. However, this drawback of using hyperbolic-trigonometric displacement shape functions is overcome by the improved accuracy of the proposed model as shown in the following numerical results. A midspan vertical load is applied proportionally under displacement-control

marching scheme. Fig 4(a) presents the responses obtained with different meshes of the proposed Winkler-based beam element. This plot indicates that 8 elements are sufficient to obtain the benchmark response, with 4 elements yielding already a satisfactory response. Two drastic changes in the response stiffness are caused first by yielding of the beam section and next by yielding of the foundation springs. Fig 4(b) shows the convergence study of the displacement-based model proposed by Limkatanyu and Spacone (2006). It is seen that 16 elements are needed to obtain the benchmark response, thus indicating that the improved displacement shape functions derived in the present work can greatly enhance the model accuracy. It is worth mentioning that the convergence study performed in Limkatanyu and Spacone (2006) indicated that two force-hybrid elements were needed to obtain the benchmark response while four mixed elements were required to obtain the same response. However, the displacement Winkler-based model proposed herein does not require the complex element state determination as needed in the force-hybrid and mixed models. Therefore, it can easily be implemented in the standard finite-element analysis platform. Furthermore, it is clear that for the linear elastic response where the midspan deflection is less than 0.0115 m, only one proposed beam element is sufficient to obtain the benchmark response while four beam elements with cubic Hermitian polynomials are required to give the same degree of accuracy. It is noted that both averaging schemes (Eqs. (27) and (28)) to determine the average value of λ used do not lead to different results. This is due to the fact that both beam-section and foundation responses are described by the bilinear function and the integration-point and element numbers are sufficient to make this local effect irrelevant.

To further demonstrate the superiority of the proposed model, local convergence studies are also performed. In order to obtain the more accurate local force and deformation distributions, the numbers of elements are doubled from 8 to 16 for the proposed model and from 32 to 64 for the model proposed by Limkatanyu and Spacone (2006). Respectively, Figs. 5(a) and (b) show the distributions of beam curvature and beam moment at integration points along the beam length associated with a midspan deflection δ=0.1 m. For the displacement-based model of Limkatanyu and Spacone (2006), there are apparent discontinuities in the curvature distributions between adjacent elements, especially along the beam portions where plastic hinges are formed. This is due to the weak satisfaction of element equilibrium. However, the jump in the moment distribution between adjacent elements is rather small in Fig. 5(b) and is not clearly visible. For the displacement-based model proposed in the present study, there is continuity in the curvature distributions between adjacent elements even though the element equilibrium is also satisfied in the weak sense. This is due to the improved nature of the analytically derived displacement shape functions. It is noted that the Gauss-Lobatto integration scheme is used in the element implementation, thus each of the two beam elements sharing a node has a monitored section located at the nodal coordinates. It is worth mentioning that similar discontinuities in curvature and moment

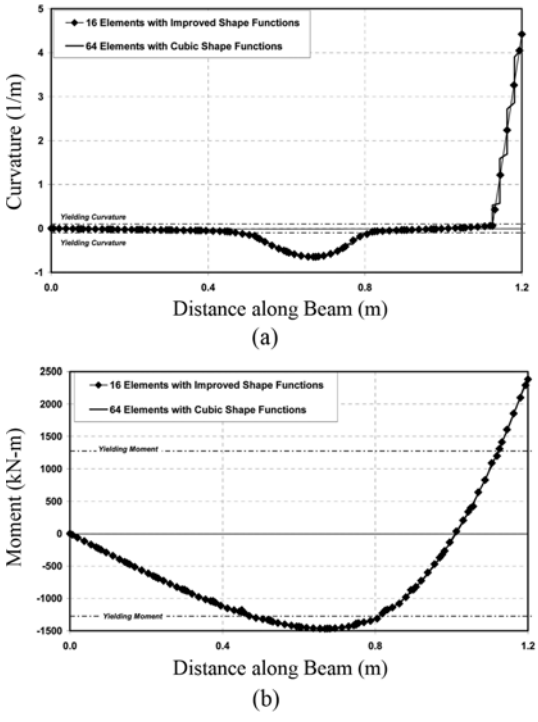

Fig. 5. Curvature and Moment Distributions along the Beam for Midspan Displacement δ = 0.1 m

distributions were also found for the two-field mixed element proposed by Limkatanyu and Spacone (2006). This is, however, the result of condensation of the nodal force degrees of freedom during element implementation. Respectively, Figs. 6(a) and (b) show the distributions of the foundation deformation and force at the integration points along the beam length associated with a midspan deflection δ=0.1 m. For both displacement-based models, there is continuity in the foundation-deformation (vertical deflection) and the foundation-force distributions between adjacent elements because the foundation-compatibility equation is imposed in a point-wise sense. It is worth mentioning that for the force-hybrid element proposed by Limkatanyu and Spacone (2006), there exist discontinuities in the foundation-deformation and the foundation-force distributions between adjacent elements because the reference foundation forces are condensed out during element implementation. The results shown Figs. 5 and 6 clearly and conclusively indicated that the accuracy of proposed model is superior both at the global (Fig. 4) and local levels.

5.2 Example II: Softening Beam-Foundation System

The free-free beam on the Winkler foundation subjected to a concentrated load at its midspan is shown in Fig. 7. This beam-foundation system is employed to demonstrate the capability of the proposed beam element to trace the softening response due to softening of the supporting foundation. Therefore, the hardening foundation of the beam used earlier is replaced by a softening foundation. The softening branch of the foundation force-deformation relation is assumed to be linear. The yield displacement is 0.04 m associated with a 40-kN/m-yield force and the ultimate

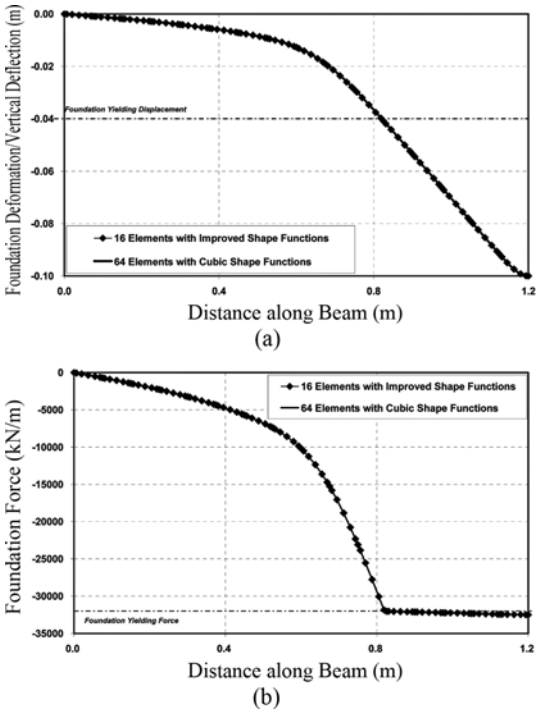

Fig. 6. Foundation Deformation and Force Distributions along the Beam for Midspan Displacement δ = 0.1 m

displacement is 0.08 m associated with zero resistance. Thirty two proposed beam elements are used to discretize the whole beam (16 elements per each half). It is noted that a finer mesh was used to model this beam-foundation system but it yielded basically the same results. Therefore, the strain localization is not a concern in this particular system. However, in other cases with a strain-softening section response the prediction could become mesh-dependent and the mesh should be carefully selected. A midspan vertical displacement is imposed proportionally under displacement-control. The midspan load-displacement diagram is shown in Fig. 8. In the figure, six loading points are associated with different responding scenarios: Point A with the formation of the first plastic hinge (positive moment); Point B with the first yielding of the foundation; Point B* with the peak of resisting

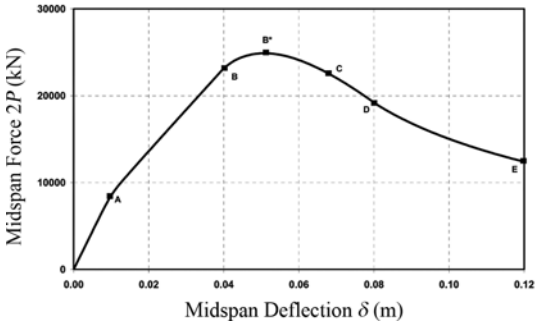

Fig. 8. Load-Displacement Response of Free-Free Beam on Softening Foundation

forces; Point C with the formation of the second plastic hinges (negative moment); Point D with the first loss of the foundation resistance; and Point E with a midspan deflection δ=0.12 m. Figs. 9(a) and (b) show the distributions of the beam curvature and beam moment at the integration points along the beam length associated with the loading points A to E. Figs. 10(a) and (b) show the distributions of the foundation deformation and force at the integration points along the beam length associated with the loading points A to E. It is interesting to observe that even though the foundation starts to soften at Point B, the beam-foundation does not immediately lose its loading capacity. Instead, it can carry further applied loads until it reaches the peak at Point B* where the central portion of the foundation (around 0.4 m) is in the softening branch. This is due to the statically indeterminate nature inherent to the system. From points B* to C, even though the system is unloading globally, certain portions of the beam are loading locally, resulting in the formation of plastic hinges at x=0.68 m and 1.72 m. From points D to E, the complete loss of the foundation resistance initiates at the midspan and propagates toward the free ends. As observed in Fig. 9, the locations of maximum negative moments tend to shift outward to the free ends. Due to the complete loss of supporting foundation at the central portion of the beam, the positive moments drastically increase and rapidly propagate toward the free ends. The results of the investigation on local responses show the ability of the model to represent the internal-force redistri-

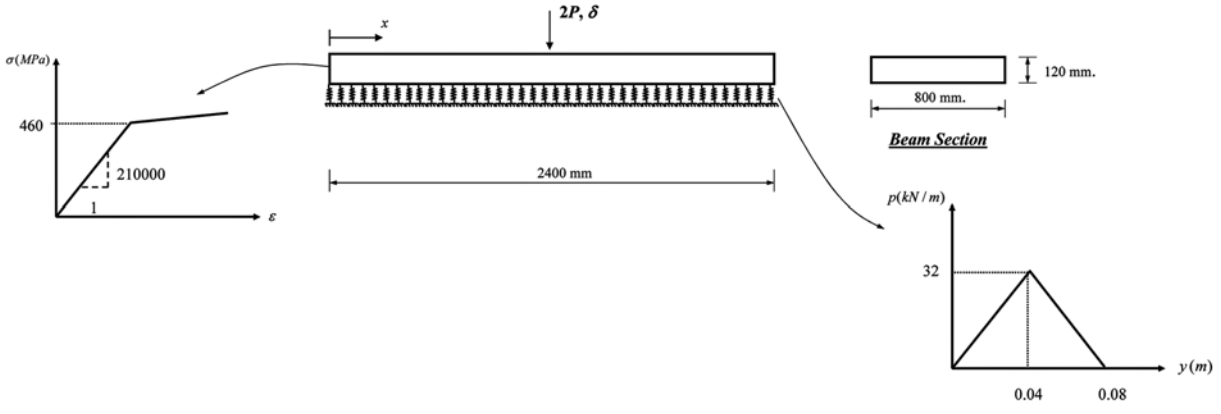

Fig. 7 Example II: Free-Free Beam on Softening Foundation

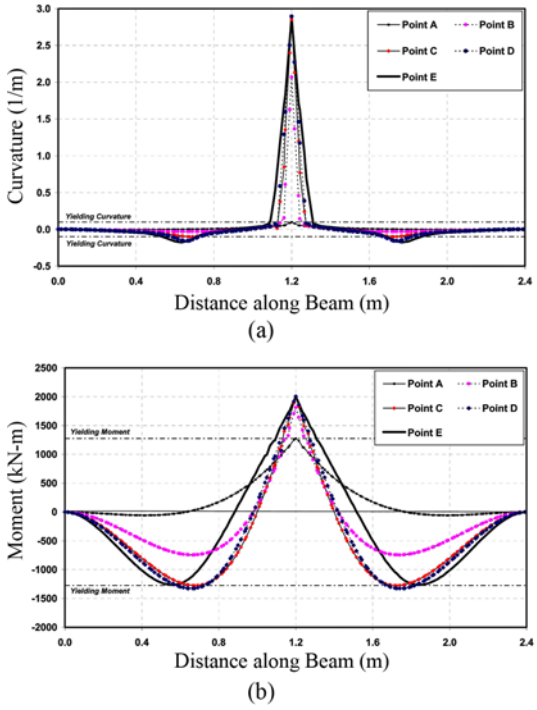

Fig. 9. Curvature and Moment Distributions along the Beam for Different Loading Scenarios in Fig. 8

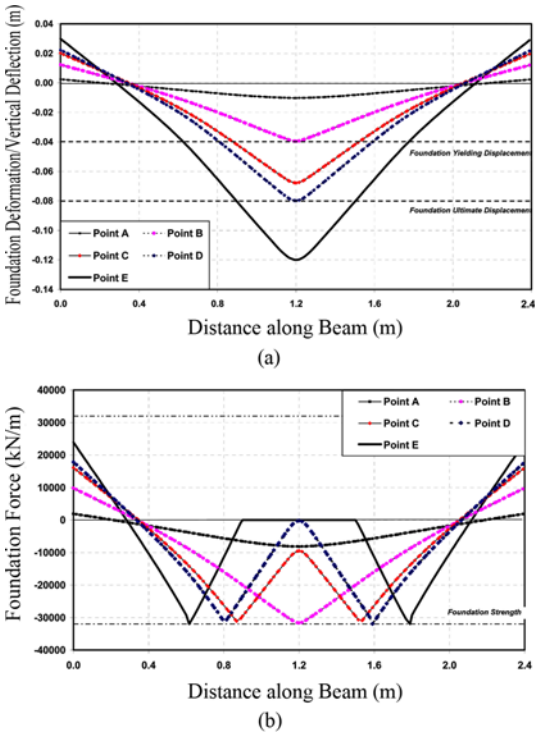

Fig. 10. Foundation Deformation and Force Distributions along the Beam for Different Loading Scenarios in Fig. 8

bution nature inherent to the beam-foundation system.

6. Conclusions

This paper presents a new nonlinear Winkler-based beam element. The element formulation is based on virtual displacement principle using improved displacement shape functions. The improved displacement shape functions are obtained by solving analytically the governing differential equilibrium equation. Two numerical examples are analyzed using the proposed model. The first numerical example confirms the superiority of the proposed model over ones previously proposed in the literature. This is conceived fortunately by the improved nature of the analytically derived displacement shape functions. The second example shows the success of the proposed model in tracing the softening response of the beam with the softening foundation and in representing the internal-force redistribution capacity inherent to the beam-foundation system. The development of the proposed Winkler-based beam element is a step forward in establishing a computational framework that permits a full nonlinear analysis of frame structures including the soil-structure interaction effects (e.g., shallow foundation rocking).

Acknowledgements

This study was partially supported by the Thai Ministry of University Affairs (MUA), by the Thailand Research Fund (TRF) under Grant MRG4680109 and Grant RSA5480001, by STREAM Research Group under Grant ENG-51-2-7-11-022-S, Faculty of Engineering, Prince of Songkla University, and by a grant (11 cutting-edge urban C10) from Cutting-edge Urban Development Program funded by Ministry of Land, Transport and Maritime Affairs of Korean. Any opinions expressed in this paper are those of the authors and do not reflect the views of the sponsoring agencies. Special thanks go a senior lecturer Mr. Wiwat Sutiwipakorn for reviewing and correcting the English of this paper. In addition, the authors would also like to thank two anonymous reviewers for their valuable and constructive comments.

References

Avramidis, I. E. and Morfidis, K. (2006). "Bending of beams on three-parameter elastic foundation." *Int. J. Solids. Struct.*, Vol. 43, No. 2, pp. 357-375.

Bowles, J. E (1974). *Analysis and computer methods in foundation engineering*, McGraw Hill, New York.

Celep, Z. and Demir, F. (2007). "Symmetrically loaded beam on a two-parameter tensionless foundation." *Struct. Eng. Mech.*, Vol. 27, No. 5, pp. 555-574.

Chore, H. S., Ingle, R. K., and Sawant, V. A. (2010). "Building frame-pile foundation-soil interaction analysis: A parametric study." *Interact. Multiscale Mech.,* Vol. 3, No. 1, pp. 55-79.

Eisenberger, M. and Yankelevsky, D. Z. (1985). "Exact stiffness matrix for beams on elastic foundation." *Comput. Struct.*, Vol. 21, No. 6, 1355-1359.

Gendy, A. S. and Saleeb, A. F. (1999). "Effective modeling of beams with shear deformations on elastic foundation." *Struct. Eng. Mech.*, Vol. 8, No. 6, pp. 607-622.

Gosowski, B. (2007). "Non-uniform torsion of stiffened open thin-walled members of steel structures." *J. Constr. Steel Res.*, Vol. 63, No. 6, pp. 849-865.

Harden, C. W. and Hutchinson, T. C. (2009). "Beam-on-nonlinear-Winkler-foundation modeling of shallow rocking-dominated footings." *Earthq. Spectr.*, Vol. 25, No. 2, pp. 277-300.

He, X. G. and Kwan, A. K. H. (2001). "Modeling dowel action of reinforcement bars for finite element analysis of concrete structures." *Comput. Struct.*, Vol. 79, No. 6, pp. 595-604.

Hetenyi, M. (1946). *Beams on elastic foundations*, University of Michigan Press, Ann Arbor, M.I.

Kerr, A. D. (1965). "A study of a new foundation model." *Acta Mech.*, Vol. 1, No. 2, pp. 135-147.

Kim, S. M. and Chung, W. (2009). "Vibration of simplified prestressed pavement model under moving two-axle harmonic loads." *KSCE. J. Civ. Eng.*, Vol. 13, No. 6, pp. 409-421.

Kim, S. M. and Yang, S. (2010). "Moving two-axle high frequency harmonic loads on axially loaded pavement systems." *KSCE. J. Civ. Eng.*, Vol. 14, No. 4, pp. 513-526.

Lee, B. K., Kim, S. K., Lee, T. E., and Ahn, D. S. (2003). "Free vibrations of tapered beams laterally restrained by elastic springs." *KSCE. J. Civ. Eng.*, Vol. 7, No. 2, pp. 193-199.

Limkatanyu, S., Kwon, M., Prachasaree, W., and Chaiviriyawong, P. (2012). "Contact-interface fiber-section element: shallow foundation modeling." *Geomech. Eng.*, Vol. 4, No. 3, pp. 173-190.

Limkatanyu, S. and Spacone, E. (2006). "Frame element with lateral deformable supports: Formulations and numerical validation." *Comput. Struct.*, Vol. 84, Nos. 13-14, pp. 942-954.

Ma, X., Butterworth, J. W., and Clifton, G. C. (2009). "Static analysis of an infinite beam resting on a tensionless Pasternak foundation." *Eur. J. Mech. A-Solid*, Vol. 28, No. 4, pp. 697-703.

Matlock, H. and Reese, L. C. (1960). "Generalized solutions for laterally loaded piles." *J. Soil Mech. Found. Div. ASCE.*, Vol. 86, No. 5, pp. 63-91.

Mindlin, R. D. (1936). "Force at a point in the interior of a semi-infinite solid." *Physics*, Vol. 7, pp. 195-202.

Miranda, C. and Nair, K. (1966). "Finite beams on elastic foundation." *J. Struct. Div. ASCE.*, Vol. 92, pp. 131-142.

Mullapudi, R. and Ayoub, A. (2010). "Nonlinear finite element modeling of beams on two-parameter foundations." *Comput. Geotech.*, Vol. 37, No. 3, pp. 334-342.

Pilkey, W. D. (2007), *Analysis and design of elastic beams: Computational methods*, John Wiley & Sons Inc., New York.

Raychowdhury, P. (2011). "Seismic response of low-rise Steel Moment-Resisting Frame (SMRF) buildings incorporating nonlinear Soil-Structure Interaction (SSI)." *Eng. Struct.*, Vol. 33, No. 3, pp. 958-967.

Reissner, E. (1967). "Note on the formulation of the problem of the plate on an elastic foundation." *Acta Mech.*, Vol. 4, No. 1, pp. 88-91.

Sapountzakis, E. J. and Kanpitsis, A. E. (2010). "Nonlinear dynamic analysis of Timoshenko beam-columns partially supported on tensionless Winkler foundation." *Comput. Struct.*, Vol. 88, Nos. 21-22, pp. 1206-1219.

Sapountzakis, E. J. and Kanpitsis, A. E. (2011a). "Nonlinear response of shear deformable beams on tensionless nonlinear viscoelastic foundation under moving loads." *J. Sound Vib.*, Vol. 330, No. 22, pp. 5410-5426.

Sapountzakis, E. J. and Kanpitsis, A. E. (2011b). "Nonlinear analysis of shear deformable beam-columns partially supported on tensionless three-parameter foundation." *Arch. Appl. Mech.*, Vol. 81, No. 12, pp. 1833-1851.

SEAOC (1995). *Vision 2000: Performance based seismic engineering of buildings*, Structural Engineers Association of California, Sacramento, CA.

Selvadurai, A. P. S. (1979). *Elastic analysis of soil-foundation interaction*, Elsevier Publishing Company, Inc., New York.

Shokrieh, M.M. and Heidari-Rarani, M. (2011). "A comparative study for beams on elastic foundation models to analysis of mode-I delamination in DCB specimens." *Struct. Eng. Mech.*, Vol. 37, No. 2, pp. 149-162.

Taciroglu, E., Rha, C. S., and Wallace, J. W. (2006). "A robust marco-element model for soil-pile interaction under cyclic loads." *J. Geotech. Geoenviron. Eng.,* Vol. 132, No. 10, pp. 1304-1314.

Taylor, R. L. (2000). *FEAP: A finite element analysis program*, User Manual: Version 7.3, Department of Civil and Environmental Engineering, University of California, Berkeley.

Ting, B. Y. and Mockry, E. F. (1984). "Beam on elastic foundation finite elements." *J. Struct. Div. ASCE.,* Vol. 110, No. 10, pp. 2324-2339.

Tong, P. and Rossettos, J. N. (1977). *Finite element method: Basic technique and implementation*, MIT Press, Cambridge.

Vlasov, V. Z. and Leontiev, U. N. (1966). *Beams, plates, and shells on elastic foundation*, Israel Program for Scientific Translations, Jerusalem (Translated from Russian).

Wang, X. Y. and Chen, W. (2010). "The coupled vibration of fluid-filled multiwalled carbon nanotubes with intertube deformation." *J. Appl. Phys.*, Vol. 108, No. 11, pp. 1-13.

Winkler, E. (1867). *Die lehre von der elastizität und Festigkeit*, Prag.

Wolfram, S. (1992). *Mathematica reference guide*, Addison-Wesley Publishing Company, Redwood City.

Zhang, Y. (2009). "Tensionless contact of a finite beam resting on Reissner foundation." *Int. J. Mech. Sci.*, Vol. 50, No. 5, pp. 1035-1041.

Zhang, L., Zhao, M., Zou X., and Zhao, H. (2009). "Deformation analysis of geocell reinforcement using Winkler model." *Comput. Geotech.*, Vol. 36, No. 6, pp. 977-983.

Appendix. Displacement Shape Functions, Curvature-displacement Shape Functions, and Foundation Deformation-displacement Shape Functions

The displacement shape functions may be written as:

$$N_{B1}(x)=\frac{\phi_2\cos(2L-x)\lambda+\phi_3\cos\lambda x-\phi_4\sin(2L-x)\lambda+\phi_5\sin\lambda x}{2\phi_1} \tag{29}$$

$$N_{B2}(x)=\frac{\phi_4\cos(2L-x)\lambda-\phi_4\cos\lambda x+(e^{2\lambda L}-1)\phi_6\sin\lambda x}{2\lambda\phi_1} \tag{30}$$

$$N_{B3}(x)=\frac{\phi_8\cos(L-x)\lambda+\phi_9\cos(L+x)\lambda+\phi_{10}\sin(L-x)\lambda-\phi_6\sin(L+x)\lambda}{\phi_7} \tag{31}$$

$$N_{B4}(x)=\frac{\phi_6\cos(L-x)\lambda-\phi_6\cos(L+x)\lambda-(e^{2\lambda L}-1)\phi_{11}\sin(L-x)\lambda}{\lambda\phi_7} \tag{32}$$

The curvature-displacement shape functions may be written as:

$$B_{B1}(x)=\frac{\lambda^2(\phi_2\cos(2L-x)\lambda-\phi_{12}\cos\lambda x+\phi_4\sin(2L-x)\lambda+\phi_{13}\sin\lambda x)}{\phi_1} \tag{33}$$

$$B_{B2}(x)=\frac{\lambda((1-e^{2\lambda L})\phi_9\cos\lambda x+\phi_2(\sin(2L-x)\lambda+\sin\lambda x))}{\phi_1} \tag{34}$$

$$B_{B3}(x)=-\frac{2\lambda^2\begin{pmatrix}(\phi_8+2\phi_9)\cos(L-x)\lambda-\phi_9\cos(L+x)\lambda\\-(\phi_{10}+2\phi_6)\sin(L-x)\lambda-\phi_6\sin(L+x)\lambda\end{pmatrix}}{\phi_7} \tag{35}$$

$$B_{B4}(x)=\frac{2\lambda((e^{2\lambda L}-1)\phi_{14}\cos(L-x)\lambda-2\phi_9\sin\lambda L\cos\lambda x)}{\phi_7} \tag{36}$$

The foundation deformation-displacement shape functions may be written as:

$B_{s1}(x)=N_{B1}(x)$; $B_{s2}(x)=N_{B2}(x)$; $B_{s3}(x)=N_{B3}(x)$; $B_{s4}(x)=N_{B4}(x)$

where,

$$\phi_1=\frac{-2+\cos2\lambda L+\cosh2\lambda L}{e^{-(x+2L)\lambda}}\ ;\ \phi_2=e^{2\lambda L}+e^{2\lambda(L+x)}\ ;$$

$$\phi_3=-2e^{2\lambda L}+e^{4\lambda L}+e^{2\lambda x}-2e^{2\lambda(L+x)}\ ;\ \phi_4=e^{2\lambda L}(-1+e^{2\lambda x})\ ;$$

$$\phi_5=e^{4\lambda L}-e^{2\lambda x}\ ;\ \phi_6=e^{2\lambda L}-e^{2\lambda x}\ ;\ \phi_7=\frac{1+e^{4\lambda L}+2e^{2\lambda L}(-2+\cos2\lambda L)}{e^{\lambda(L-x)}}\ ;$$

$$\phi_8=1+e^{2(L+x)\lambda}-2(e^{2\lambda L}+e^{2\lambda x})\ ;\ \phi_9=e^{2\lambda L}+e^{2\lambda x}\ ;$$

$$\phi_{10}=e^{2(L+x)\lambda}-1\ ;\ \phi_{11}=-1+e^{2\lambda x}\ ;\ \phi_{12}=e^{4\lambda L}+e^{2\lambda x}\ ;$$

$$\phi_{13}=-2e^{2\lambda L}+e^{4\lambda L}-e^{2\lambda x}+2e^{2(L+x)\lambda}\ ;\text{ and }\ \phi_{14}=1+e^{2\lambda x} \tag{37}$$